Representation of the Visual Field in the Human Occipital Cortex

A Magnetic Resonance Imaging and Perimetric Correlation

Agnes M. F. Wong, MD; James A. Sharpe, MD

Objectives: To evaluate the retinotopic map of the human occipital cortex by correlating magnetic resonance imaging (MRI) findings with visual field defects in patients with occipital lobe infarcts and to assess the compatibility between our cliniconeuroimaging findings and the location of lesions predicted by the classic Holmes map and a revised map.

Methods: Magnetic resonance images were obtained in 14 patients with occipital lobe infarcts. Visual field analysis was performed with tangent screen, the Goldmann perimeter, and the Humphrey Field Analyzer. Based on the pattern of visual field deficit, the location of the lesion in the mesial occipital lobe in each patient was predicted using the Holmes map and other retinotopic maps of the occipital cortex. The predicted location of the lesion was then compared with its actual location shown on MRI to assess the compatibility between our data and the other maps. These maps determine retinotopic correlates of the medial occipital lobe, but they cannot establish correlates of the striate cortex (V1). The medial occipital representation of central vision was evaluated by regression analysis.

Results: The MRI correlations in this study confirmed gross estimates of the retinotopic organization of the occipital cortex. However, our findings did not correlate exactly with the Holmes map. We determined that the central 15° of vision occupies 37% of the total surface area of the human medial occipital lobe. Based on our data, a refined retinotopic map is presented.

Conclusions: The resolution of conventional MRI testifies to its considerable value in localizing occipital lobe lesions. Our findings support, and refine, the Holmes map of the human occipital cortex.

Arch Ophthalmol. 1999;117:208-217

From the Division of Neurology and the Department of Ophthalmology, The Toronto Hospital and the University of Toronto, Toronto, Ontario.

MUCH OF our knowledge of the representation of the visual field in the human occipital cortex was derived from studies of patients with penetrating injuries to the head during wartime. Inouye,[1] Holmes and Lister,[2] Holmes,[3,4] and, later, Spalding[5] correlated visual field deficits with the location of missile wounds in the occiput and produced retinotopic maps of the striate cortex.

The map presented by Holmes[4] is widely adopted as a detailed representation of the visual field in the human striate cortex. It depicts a point-to-point localization of the contralateral hemifield of vision in the striate cortex. The upper field is represented in the inferior calcarine cortex, and the lower field is represented in the superior cortex. The central field occupies the posterior pole, whereas the peripheral field is mapped anteriorly.[4] The macula, which subserves central vision, has a disproportionately large cortical representation[4]—up to 25% of the surface area of the striate cortex has been assigned to the central 15° of vision.[6]

The accuracy of the Holmes map was later supported by activation study of the visual cortex using positron emission tomography scanning[7] and by cliniconeuroimaging correlation using computed tomography (CT).[8-11] Spector et al,[11] using CT to study patients with occipital lobe infarction, reported a good match between cliniconeuroimaging findings and the location of lesions predicted by the Holmes map. However, these studies were limited by the resolution of early CT scans. With the introduction of magnetic resonance imaging (MRI), Horton and Hoyt[6] reexamined the Holmes map. By correlating MRI findings with homonymous field deficits in 3 patients with occipital lobe lesions, they found that the Holmes map did not correlate well with their findings.

Based on their findings, together with electrophysiologic data on Old World primates—which showed that in macaque

PATIENTS AND METHODS

Consecutive patients with visual field defects and occipital lobe lesions seen in the neuro-ophthalmology clinic at The Toronto Hospital, Toronto, Ontario, were screened using the central 30-2 threshold program of the Humphrey Field Analyzer (Allergan-Humphrey Instruments, San Leandro, Calif). Patients with incomplete homonymous hemianopia were included in the study. The central 30-2 program only tests the retinal threshold at 76 predetermined points within the central 30° of vision, with 19 points tested in each quadrant. For example, adjacent to the horizontal meridian, the tested points lie at approximately 2°, 8°, 14°, 20°, and 26° of eccentricity. Thus, the program does not provide information on the retinal threshold at approximately 3° to 7°, 9° to 13°, 15° to 19°, 21° to 25°, and 27° to 30° of eccentricity, although the gray-scale printout gives the impression that the threshold at every point is tested. In this study, all recruited patients were also tested with tangent screen and Goldmann perimetry to delineate more precisely the extent of visual field loss. If there was discrepancy among the 3 perimetric measurements, the mean value of the 3 measurements was used (in all study patients, the discrepancy among measurements was ≤5°).

Serial axial and sagittal T_1-weighted (repetition time = 516-517 milliseconds and echo time = 8-11 milliseconds) and T_2-weighted (repetition time = 2200-4383 milliseconds and echo time = 80-95 milliseconds, 2 separate acquisitions) images with a slice thickness of 5 mm were obtained in all recruited patients using the 1.5-T Signa imaging system, version 5.4.2 (General Electric Medical Systems, Milwaukee, Wis). The MR images were then processed on a workstation (SUN/SPARC 10 "Advantage Windows," General Electric Medical Systems). Patients with well-defined infarcts in the occipital cortex with a minimum duration of 3 months were included in the study. Patients with lesions that may have functional neurons remaining within the neuroimaged boundaries, such as edema or hemorrhage secondary to tumors, arteriovenous malformations, or primary intracerebral hemorrhages, were excluded. Using a software program (Advantage Window v.1.2, General Electric Medical Systems), the anterior and posterior extent of the infarct (as measured by its linear distance from the occipital pole) was independently determined by assessing T_1- and T_2-weighted images in axial (along the calcarine fissure) and midsagittal orientations by us. If there were discrepancies in measurements between T_1 vs T_2 images, orientations, or between us, the mean distance from the occipital pole was used (in all study patients, the discrepancy between measurements was ≤3 mm). Using the same software program, the infarcted and normal portions of the occipital cortex were traced out using a pointing device independently by us, and the corresponding surface areas were calculated by the planimetric program available in the software. If there was a discrepancy in measurements between us, the mean surface area was used (in all study patients, the discrepancy between measurements was ≤30 mm^2).

To assess the accuracy of the Holmes map[4] and a revised map,[6] the location of the lesion in each patient was predicted using the 2 maps based on the patient's visual field defect. We then compared the predicted location of the lesion with its actual location on MRI to assess the compatibility between our data and the 2 maps.

To evaluate the cortical representation of central vision, the percentage of the surface area of the infarcted or noninfarcted (see below) occipital cortex was plotted against the degree of eccentricity from fixation.

In patients with posterior lesions that began at the occipital pole, the surface area of the lesions was used in the analysis. For example, patient 1 (**Figure 1**), who had an inferior scotoma extending from 2° to 10°, was shown to have an infarct extending from the occipital pole to 12 mm anteriorly above the calcarine fissure by MRI, which measured 300 mm^2. Assuming the total surface area of the average human striate cortex to be about 2500 mm^2 (based on postmortem specimens and after allowing for shrinkage),[6,14] the percentage of surface area of the lesion above the calcarine fissure was calculated to be 12%, which corresponded to an eccentricity of 10°. Because the area above and below the calcarine fissure is represented at any eccentricity, 24% (12% × 2) of the total surface area was assigned to an eccentricity of 10°.

In patients with anterior lesions that began at some distance from the occipital pole, the surface area of the normal area of the occipital cortex posterior to the lesions was used. For example, patient 4 (**Figure 2**), who had an inferior quadrantanopia sparing the central 11°, was shown to have a lesion that began at 16 mm and extended anteriorly to 25 mm from the occipital pole above the calcarine fissure. The surface area of the normal cortex posterior to the lesion above the calcarine fissure was 375 mm^2, representing 15% of the total surface area and corresponding to an eccentricity of 11°. Therefore, 30% (15% × 2) of the total surface area was assigned to an eccentricity of 11°.

Regression analysis of the relationship between eccentricity from fixation and the corresponding percentage surface area of the medial occipital cortex was performed. The percentage of the area of the occipital cortex subserving the central 15° of vision was then determined. Based on the cliniconeuroimaging findings in study patients, we constructed a new retinotopic map of the human occipital cortex.

monkeys as much as 70% of the total surface area of the striate cortex is occupied by the central 15° of vision[12,13]—Horton and Hoyt[6] proposed that the cortical magnification of the human striate cortex is scaled to that in the macaque striate cortex. They concluded that the Holmes map underestimated the cortical magnification of central vision, and they proposed a revised map.[6] In that revised map,[6] the human striate cortex was approximately an ellipse measuring about 80 × 40 mm. The area subserving central vision was expanded such that approximately 70% of the total surface area of the human striate cortex was assigned to the central 15° of vision.

We correlated MRI findings with the location and extent of visual field deficits in a series of patients with occipital lobe infarcts to determine the retinotopic representation of the human occipital cortex. To assess the accuracy of the Holmes map[4] and a revised map,[6] we compared our cliniconeuroimaging findings with the locations of lesions predicted by the 2 maps. Based on the findings in our patients, the percentage of the total sur-

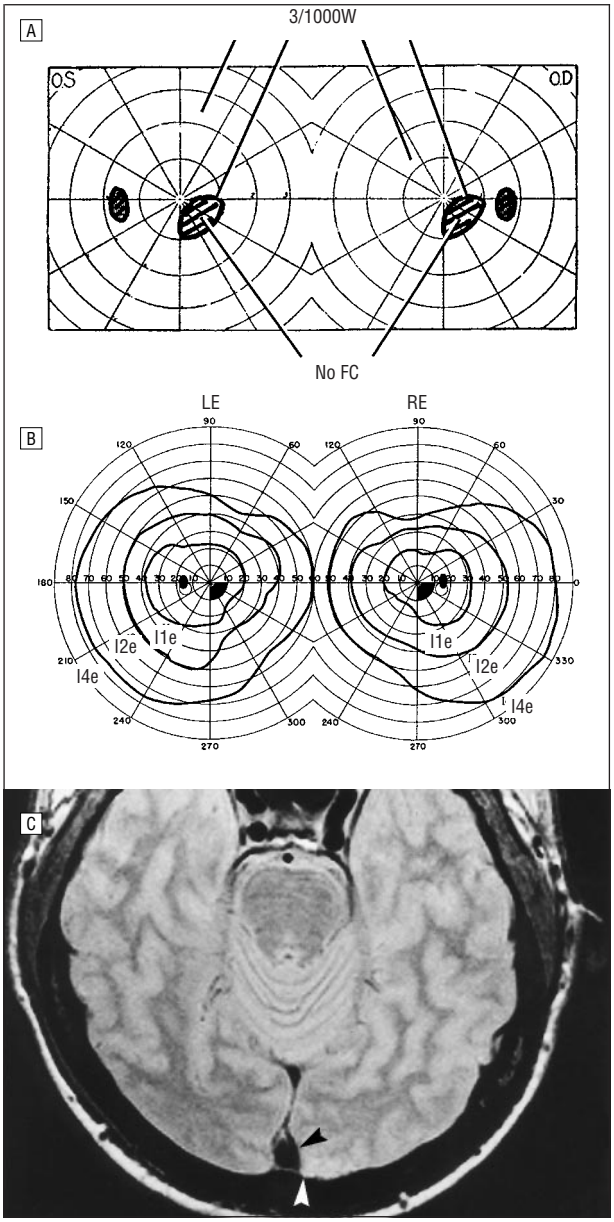

Figure 1. *Patient 1. A, Right homonymous paracentral scotoma in the lower quadrant shown by tangent screen. B, Mapping of the scotoma using Goldmann perimetry revealing the scotoma to be dense to V4e object and to extend from 2° to 10°. C, Axial T2-weighted magnetic resonance image showing a lesion beginning at the tip (white arrowhead) of the left occipital pole and extending anteriorly for 12 mm (black arrowhead). FC indicates finger counting; W, white test object.*

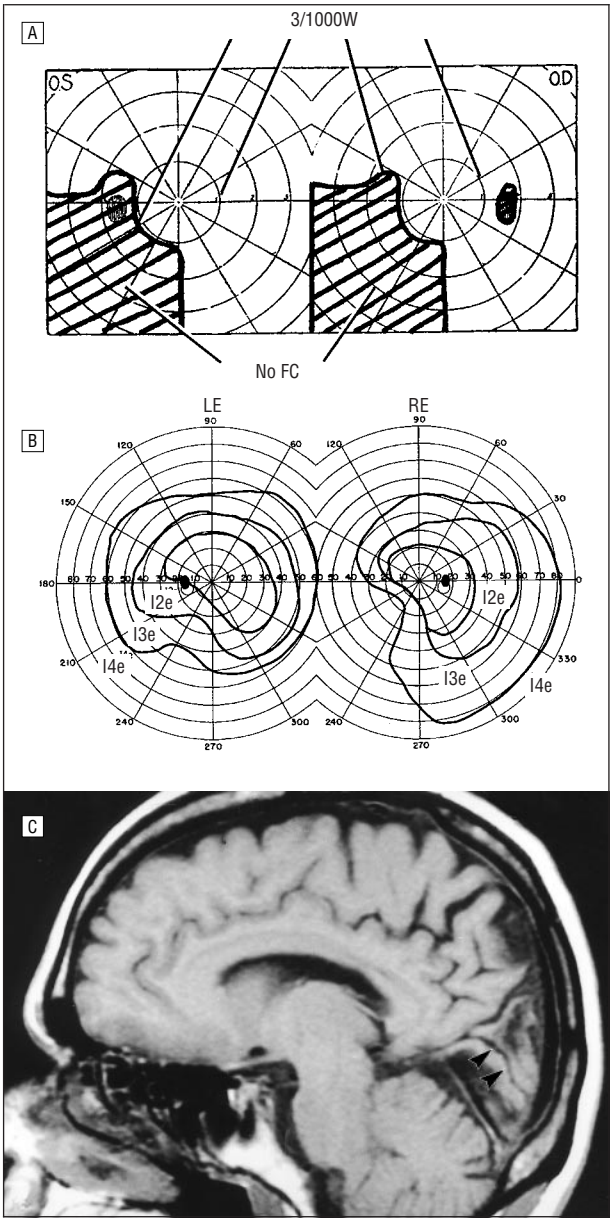

Figure 2. *Patient 4. A, Left homonymous inferior quadrantanopia shown by tangent screen. B, Mapping by Goldmann perimetry revealing sparing of central 11°, without sparing of the temporal crescent. C, Sagittal magnetic resonance image showing a lesion beginning at 16 mm and extending anteriorly to 25 mm from the right occipital pole (black arrowheads). FC indicates finger counting; W, white test object.*

face area of the medial occipital cortex devoted to central vision was estimated, and a refined retinotopic map is presented.

RESULTS

Fourteen patients had well-defined infarcts in the occipital cortex on MRI scans and were included in the analysis (**Table 1**). There were 9 males and 5 females, with ages ranging from 17 to 74 years (mean, 50 years). The mean duration of lesions was 14 months (range, 3-84 months). All 14 patients had incomplete homonymous visual field defects by Humphrey perimetry (**Figure 3**), tangent screen, and Goldmann perimetry. **Figure 4** shows the visual field defects on tangent screen, and a schematic representation of the location of the corresponding lesions, using the axial brain templates by Damasio and Damasio.[15]

The visual field defect, the locations of the lesions predicted by the Holmes[4] map and a revised map[6] based on visual field loss, and the actual locations of the lesions on MRI scans are shown in **Table 2**. For example, for patient 1, who has a right homonymous inferior quadrant scotoma from 2° to 10°, the Holmes map predicts a lesion to extend from the occipital pole to 9 mm anteriorly, whereas a revised map[6] predicts it to

Table 1. Patient Characteristics*

Patient No./ Sex/Age, y	Side of Lesion	Lesion Location on MRI, mm†	Duration of Lesion, mo	Visual Field Findings
1/M/37	Left	0-12	14	Right homonymous inferior quadrant scotoma 2°-10°
2/F/71	Right	0-18	5	Left homonymous hemianopic scotoma 0°-12°
3/M/48	Right	0-22	4	Left homonymous inferior quadrantanopia sparing central 2°
4/F/45	Right	16-25	8	Left homonymous inferior quadrantanopia sparing central 11°
5/F/21	Left	4-23	84	Right homonymous hemianopia sparing central 5°
6/F/28	Left	8-34	3	Right homonymous superior quadrantanopia sparing central 5°
7/M/80	Left	11-24	8	Right homonymous inferior quadrantanopia sparing central 9°
8/M/52	Right	10-40	3	Left homonymous inferior quadrantanopia sparing central 8°
9/M/65	Right	0-5	10	Left homonymous inferior quadrant scotoma 0°-6°
10/M/17	Left	7-31	25	Right homonymous hemianopia sparing central 5°
11/M/65	Left	2-40	16	Right homonymous superior quadrantanopia sparing central 2°
12/M/64	Right	0-2	3	Left homonymous inferior quadrant scotoma 0°-2°
13/M/74	Right	0-4	3	Left homonymous inferior quadrant scotoma 0°-6°
14/F/68	Right	9-35	5	Left homonymous inferior quadrant scotoma sparing central 6°

*MRI indicates magnetic resonance imaging.
†Distance from the occipital pole.

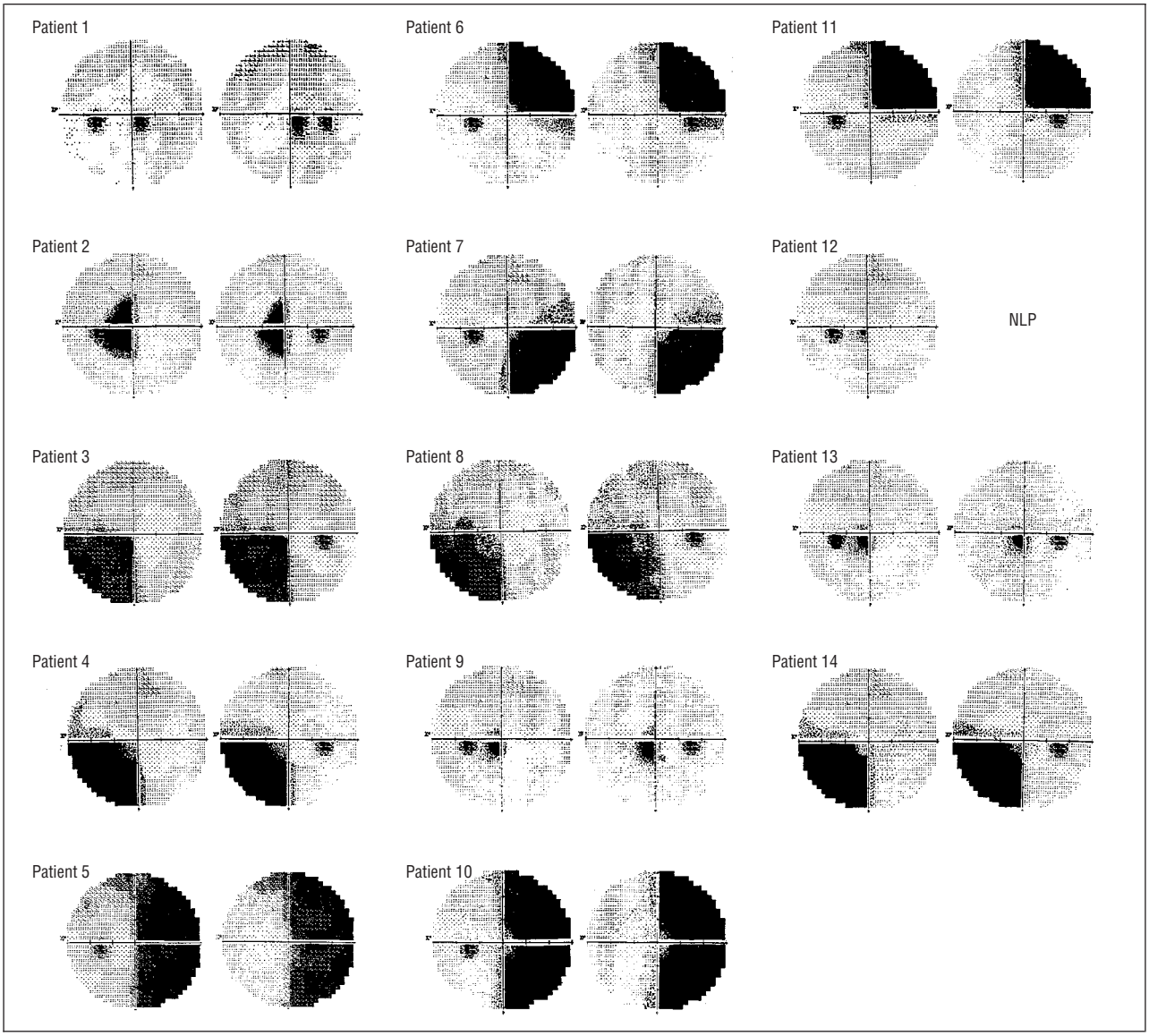

Figure 3. *Visual field defects on Humphrey automated perimetry of the 14 study patients. NLP indicates no light perception.*

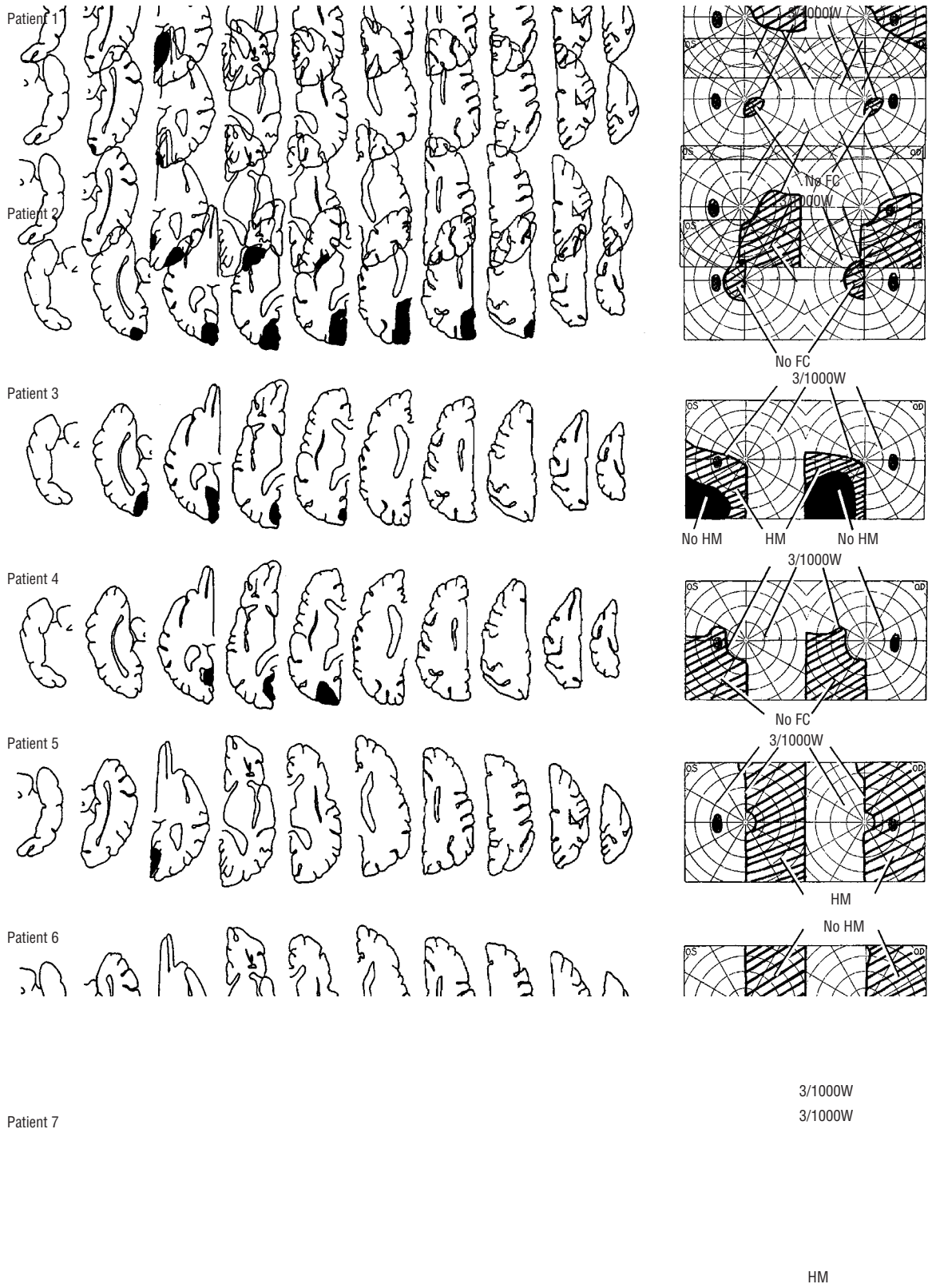

Figure 4. *Axial brain templates showing the occipital lesions of the 14 patients with their corresponding visual field defects on tangent screen. FC indicates finger counting; HM, hand movement; W, white test object; and NLP, no light perception.*

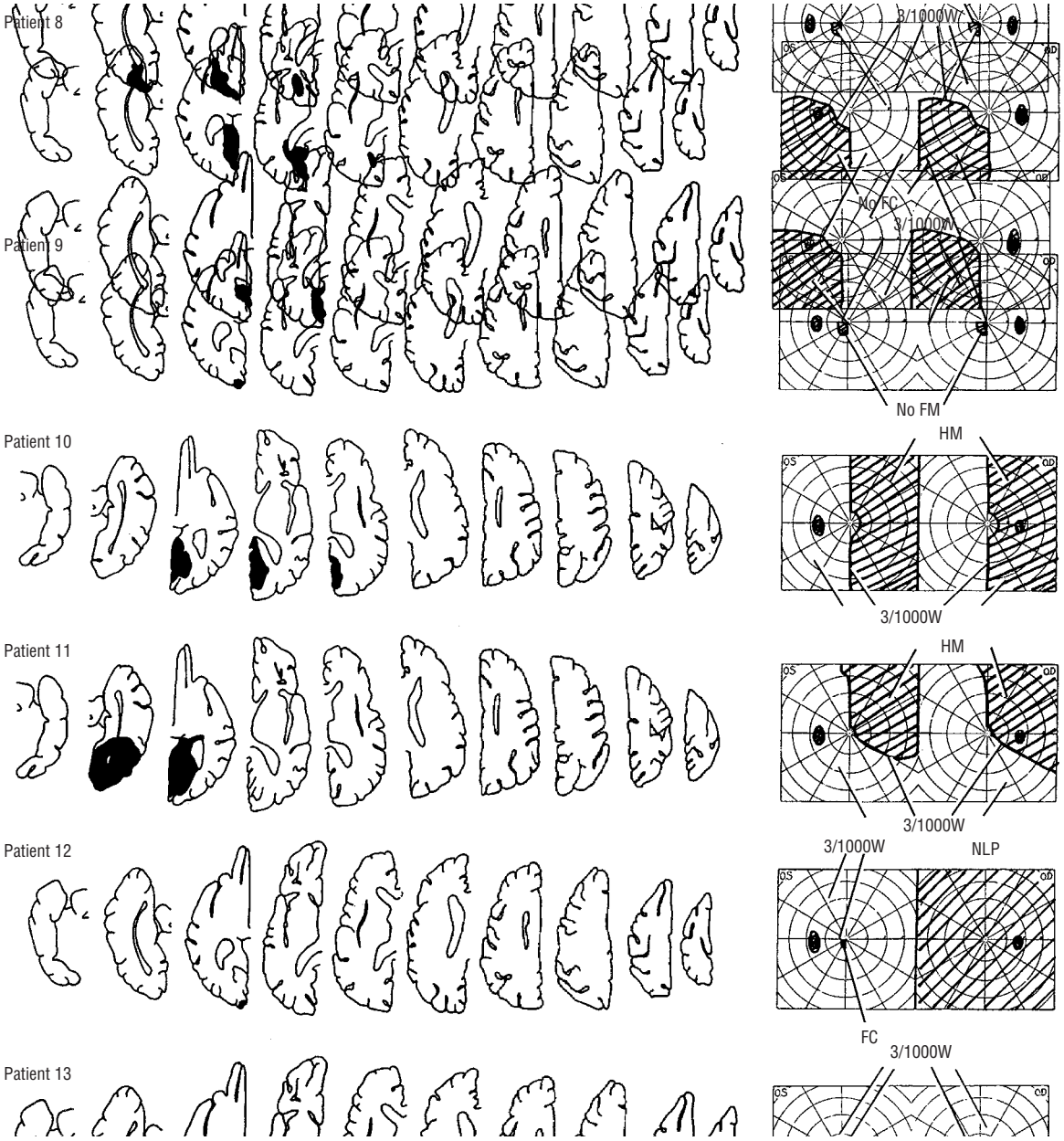
Patient 8
Patient 9
Patient 10
Patient 11
Patient 12
Patient 13
Patient 14
3/1000W
No FC
3/1000W
No FM
HM
3/1000W
HM
3/1000W
3/1000W
NLP
FC
3/1000W
FC
3/1000W
HM

Table 2. Visual Field Defects, Predicted Locations of the Lesions Based on the Holmes Map[4] and a Revised Map,[6] and the Actual Locations of the Lesions on MRIs*

Patient No.	Visual Field Findings	Predicted Lesion Location†		Location of Lesion on MRI, mm†
		Holmes Map	Revised Map	
1	Right homonymous inferior quadrant scotoma 2°-10°	0-9 mm	8-32 mm	0-12
2	Left homonymous hemianopic scotoma 0°-12°	0-13 mm	0-37 mm	0-18
3	Left homonymous inferior quadrantanopia sparing central 2°	1 mm-end	8 mm-end	0-22
4	Left homonymous inferior quadrantanopia sparing central 11°	10 mm-end	34 mm-end	16-25
5	Right homonymous hemianopia sparing central 5°	3 mm-end	22 mm-end	4-23
6	Right homonymous superior quadrantanopia sparing central 5°	3 mm-end	22 mm-end	8-34
7	Right homonymous inferior quadrantanopia sparing central 9°	8 mm-end	31 mm-end	11-24
8	Left homonymous inferior quadrantanopia sparing central 8°	7 mm-end	30 mm-end	10-40
9	Left homonymous inferior quadrant scotoma 0°-6°	0-5 mm	0-23 mm	0-5
10	Right homonymous hemianopia sparing central 5°	3 mm-end	22 mm-end	7-31
11	Right homonymous superior quadrantanopia sparing central 2°	1 mm-end	8 mm-end	2-40
12	Left homonymous inferior quadrant scotoma 0°-2°	0-1 mm	0-8 mm	0-2
13	Left homonymous inferior quadrant scotoma 0°-6°	0-5 mm	0-23 mm	0-4
14	Left homonymous inferior quadrant scotoma sparing central 6°	5-25 mm	23 to >50 mm	9-35

*MRI indicates magnetic resonance imaging; end, the juncture of the parieto-occipital and calcarine fissures.
†Distance from occipital pole.

extend from 8 mm from the occipital pole to 32 mm anteriorly. However, on MRI, the actual location of the lesion began at the occipital pole and extended to 12 mm anteriorly, which was in close agreement with the predicted location according to the Holmes[4] map. Similarly, for patient 14, who has a left homonymous inferior quadrant scotoma sparing the central 6° (**Figure 5**, A and B), the Holmes map predicts a lesion to begin at 5 mm from the occipital pole and to extend rostrally to 25 mm from the pole; on the other hand, a revised map[6] predicts it to begin at 23 mm from the occipital pole and to extend beyond 50 mm from the pole. However, on MRI (Figure 5, C), the actual lesion began at 9 mm from the occipital pole and extended to 35 mm from the pole, a finding that was in close agreement with the predicted location according to the Holmes[4] map. For the remaining 12 patients (Table 2), the locations of lesions predicted by the Holmes map were in closer agreement with their actual locations on MR images than were those predicted by a revised map.[6]

A plot of the percentage of the surface area of the infarcted or noninfarcted occipital cortex vs eccentricity from fixation is shown in **Figure 6**. The best-fit linear regression is represented by the solid line; 37% of the total surface area of the medial occipital cortex subserves the central 15° of vision.

COMMENT

Our correlations of MRI findings with visual field defects in patients with occipital lobe lesions confirmed gross estimates of the retinotopic organization of the occipital cortex. However, the visual field deficits in our patients did not correspond exactly to the Holmes map,[4] and they did not correlate with a revised map,[6] which was based on findings in 3 other reported patients. In addition, we found that 37% of the total surface area of the medial occipital cortex subserves the central 15° of vision.

From the visual field and imaging findings in our patients, a refined retinotopic map is presented (**Figure 7**). Figure 7 illustrates that the human occipital cortex is situated along the superior and inferior lips of the calcarine fissure. The foveal representation is located posteriorly at the occipital pole, whereas the peripheral visual field is represented anteriorly at the juncture of the parieto-occipital and calcarine fissures. Because the extent of striate cortex (V1) is not determined by imaging, the retinotopic correlation is with MRI of the medial occipital cortex, not with the retinotopic organization of area V1.

Several limitations confound conventional MRI in correlating lesion location with visual field defects. These limitations also apply to CT imaging of occipital lesions.[8-11] First, because visual processing in the striate cortex is organized in ocular dominance columns that have a cross-sectional width of 0.4 mm,[16] 5-mm cuts that are widely used in major MRI centers may not provide sufficient resolution to determine the exact extent and location of the lesion identified by perimetry. However, because the rostral-caudal extent of lesions in our 14 patients differed more than 5 mm from a revised map,[6] which was based on MR images of 3 patients whose slice thickness was not specified,[6] limitation of slice thickness does not explain the disparate result. Second, the determination of the extent of the lesion is complicated by areas of edema surrounding the lesion, which may be difficult to differentiate from the actual area of infarction. However, all our patients were imaged many months or years (mean duration of lesions, 14 months) after the onset of visual field loss, when edema should have completely resolved. Third, tissue damage may disrupt function but be undetected by imaging. For example, patients 3 through 7 and 10 had homonymous field defects without sparing of the temporal crescent, indicating that the most anterior portion of the occipital pole should be involved. However, on MRI, no signal change was detected in the anterior medial occipital cortex, suggesting that tissue

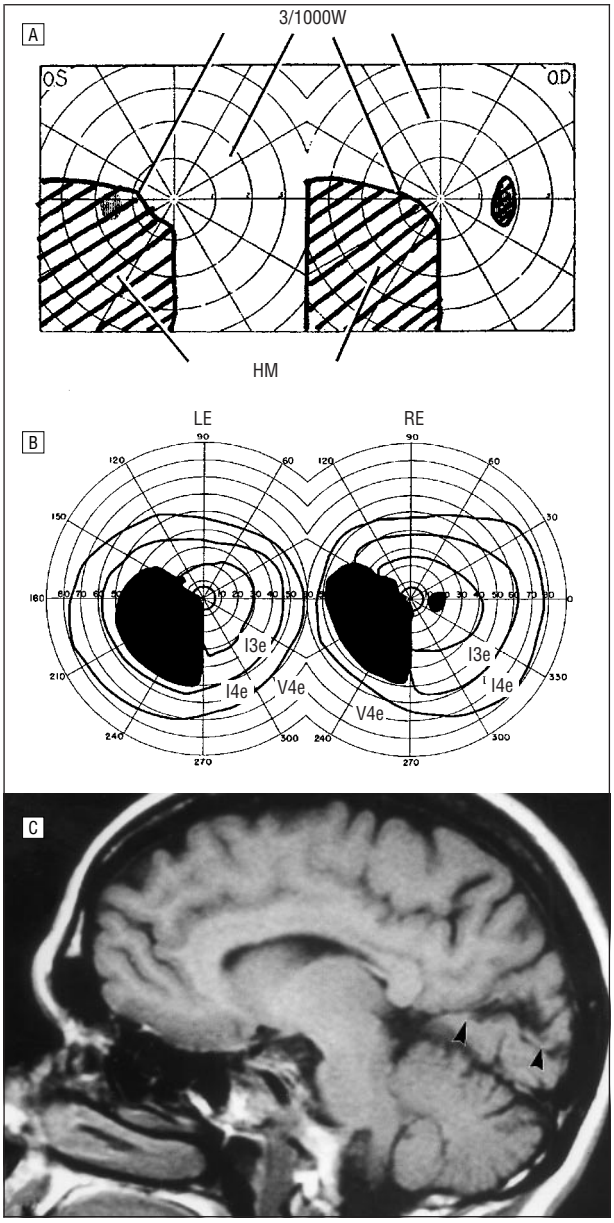

Figure 5. *Patient 14. A, Left homonymous inferior quadrant scotoma with sparing of the central 6° shown by tangent screen. B, Goldmann perimetry showing the scotoma to be dense to V4e object. C, Sagittal magnetic resonance image showing a lesion beginning at 9 mm and extending anteriorly to 35 mm from the right occipital pole (black arrowheads). HM indicates hand movemet; W, white test object.*

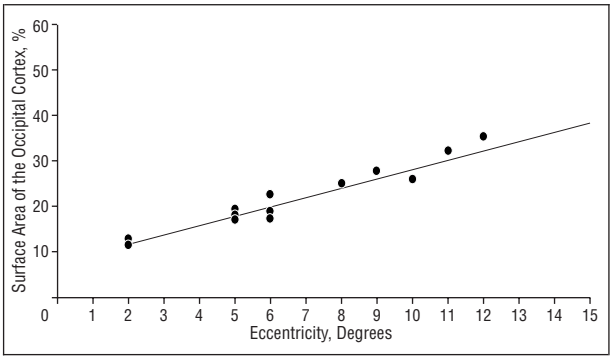

Figure 6. *Percentage of the surface area of the infarcted or noninfarcted occipital cortex vs eccentricity from fixation. The solid line represents the best-fit regression line of the values from 14 patients.*

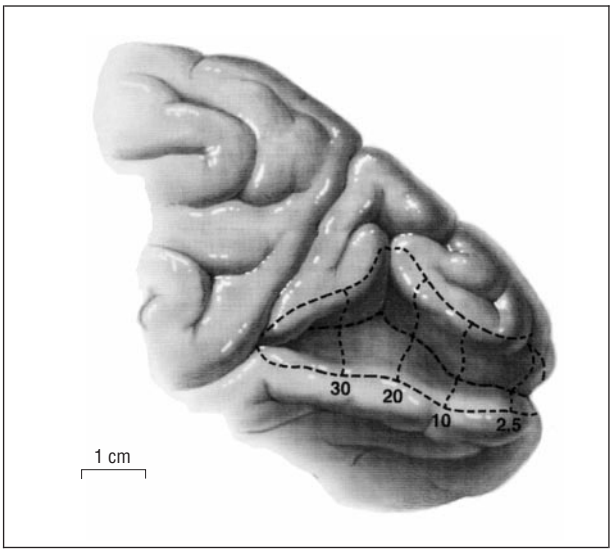

Figure 7. *Proposed retinotopic map of the occipital cortex as viewed from the mesial surface of the occipital lobe with the calcarine fissure opened. Numbers, in degrees, and the corresponding dashed lines represent visual field eccentricity along meridians. The dashed line in the calcarine fissure represents the horizontal meridian. The dashed lines at the border of the occipital cortex represent eccentricities along the lower (upper dashed line) and upper (lower dashed line) vertical meridians.*

damage may extend beyond visible MRI change; alternatively, the monocular temporal crescent of field (representing the nasal retina of the contralateral eye) may not extend to the extreme anterior part of the occipital cortex, although this seems unlikely. Fourth, areas of signal change in MRI do not specify destruction of all neural elements, which may be spared in an area of visible damage. This pertains particularly to neoplasms and hemorrhages, which we therefore excluded from our study. Fifth, because we used a 2-dimensional image to estimate the size of a 3-dimensional lesion, the accuracy of measurements depends on the orientation of the cuts. However, there is no ideal head orientation for studying the calcarine fissure because the incline of the calcarine fissure relative to other brain and skull reference coordinates is variably oriented among individuals,[17] and it also varies with minor changes in head position. Finally, and most important, the exact boundaries of the striate cortex cannot be determined by MR images, and there is a natural and substantial variation across individuals in the exact dimension and location of the striate cortex.[14] Moreover, no compensation for cortical infolding or curvature of the calcarine fissure can be made using MR images, which allows only estimation of the extent of the lesion.

The discrepancy between the results of the present study and those leading to a revised map[6] may be due in part to the small number of patients on whom a revised map was based (3 patients). In addition, whereas we excluded lesions that may have functional neurons remaining within the neuroimaged boundary, a revised map[6] included 2 patients with such lesions (1 patient had a tuberculoma and another had an arteriovenous malformation), which may lead to an overestimation of the ac-

tual area of damage. Although that revised map[6] was later supported by McFadzean and coworkers[18] using either CT or MRI in a larger series of patients, they also included 11 patients with such lesions (neoplasms, arteriovenous malformations, cerebromalacia, and hematomas). Moreover, because edema and an ischemic penumbra frequently surround the area of infarction, we only included MR images that were performed at least 3 months after patients' initial presentation, when they should have resolved. However, because previous MRI studies[6,18] did not specify the duration of lesions in their patients, bordering ischemia and edema may partly explain the disparate results.

Based on endogenous changes in magnetic susceptibility caused by localized activity-dependent variations in blood flow and oxygenation, functional MRI (fMRI) has been used to map human cortical activity during stimulation of selected areas of the visual field in normal subjects.[19-21] Sereno et al[21] and Engel et al,[22] using fMRI, found that there is emphasis on the center of gaze in the human primary visual cortex. However, their results are not consistent with our data and those from previous studies.[7-11] Potential sources of spatial spread, such as that caused by lateral neural connections within the cortex and experimental artifacts (eg, slight head movement and brain pulsatility),[22] may limit the spatial resolution of fMRI to accurately determine cortical magnification. Moreover, these studies measured a traveling wave of activity in the cortex of normal subjects by slowly changing the position of the stimuli pattern. Although these subjects were instructed to fixate at the center of the stimuli display, no attempts were made to monitor eye position during testing. Even the smallest eye movement can affect the measurement, especially at the exact center of the fovea. In addition, fMRI detects changes in signal from venous blood, not the activity of neural tissue. Some investigators[23] suggested that much of the signal change seen in fMRI might be seen within brain areas having little or no neural tissue, being instead images of the venous vasculature.

Correlation of visual field defects with neuropathologic change at autopsy may further clarify the topographic representation of the visual field in the human striate cortex.[24,25] After flattening the complete striate cortex in 4 normal adult patients with 1 eye and reconstructing the ocular dominance columns mosaic, Horton and Hocking[26] identified the blind spot representation, which lacks ocular dominance columns and extends from 12° to 18° along the horizontal meridian. They reported that 42% to 62% (mean ± SD, 52% ± 2%) of the human striate cortex corresponds to the central 12° of vision. Horton and Hoyt[6] presumed that human striate cortex and that of macaque monkeys had about the same cortical magnification of the central visual field, being 70% for the central 15°.[12,13] However, Horton and Hocking[26] reported that the cortical magnification of the central 12° of vision was 60% in monkeys and 42% to 62% (mean, 52%) in humans, an area less than that estimated in a revised map[6] and considerably smaller than that estimated by fMRI.[21] Flattening procedures[26] are subject to distortions that could affect retinotopic data. Three-dimensional MRI reconstruction of slices in different orientations may better correlate anatomy with visual field loss. Although the boundaries of striate cortex are not defined by neuroimaging methods, imaging correlates of lesions with visual field defects provide in vivo information about the retinotopic representation of vision in the occipital lobe.

The primary aim of this study was to establish a direct link between the anatomy of the medial occipital cortex along the calcarine fissure and the visual field locus and the extent of functional deficit. However, there is a limited causal relationship between the individual vagaries of the calcarine anatomic features and the retinotopic characteristics of a visual field defect. A more accurate and direct relationship is more likely to be between the location of cortical neurons receiving input from restricted receptive field positions in the retina and the location of a lesion with respect to those neurons. The arrangement of cortical neurons with respect to the gross anatomy of the calcarine fissure can be quite variable. Fundamentally, then, anatomically based retinotopic maps proposed by Holmes,[4] others,[1,5,6] and us are limited in their accuracy. However, the location of lesions within the medial occipital cortex on imaging studies has substantial value in determining whether the pattern of a patient's visual field defect is adequately accounted for by imaging. Establishing the validity of the existing retinotopic maps based on lesion data therefore becomes important to account for the symptoms of occipital cortex lesions.

Our MRI correlations confirmed estimates of the retinotopic organization of the medial occipital cortex and corresponded better with the Holmes[4] map than with a revised map[6] based on conventional MRI correlations of lesions in 3 other reported patients. Thirty-seven percent of the total surface area of the mesial surface of the human occipital cortex subserves the central 15° of vision. Although precise knowledge of the retinotopic representation of the human striate cortex (V1) is limited by imaging techniques, the resolution of MRI testifies to its considerable value in diagnosing and localizing occipital lobe lesions.

Accepted for publication September 22, 1998.

This study was supported by grant MT 5404 from the Medical Research Council of Canada.

We thank David Mikulis, MD, for his expert advice.

Reprints: James A. Sharpe, MD, Division of Neurology, The Toronto Hospital, EC 5-042, 399 Bathurst St, Toronto, Ontario, Canada M5T 2S8.

REFERENCES

1. Inouye T. *Die Sehstorungen bei Schussverletzungen der kortikalen Sehsphare.* Leipzig, Germany: W Engelmann; 1909.
2. Holmes G, Lister WT. Disturbances of vision from cerebral lesions with special reference to the cortical representation of the macula. *Brain.* 1916;39:34-73.
3. Holmes G. Disturbances of vision by cerebral lesions. *Br J Ophthalmol.* 1918;2: 353-384.
4. Holmes G. The organization of the visual cortex in man. *Proc R Soc Lond B Biol Sci.* 1945;132:348-361.
5. Spalding JMD. Wounds of the visual pathway, II: the striate cortex. *J Neurol Neurosurg Psychiatry.* 1952;15:169-183.

6. Horton JC, Hoyt WF. The representation of the visual field in human striate cortex: a revision of the classic Holmes map. *Arch Ophthalmol.* 1991;109: 816-824.
7. Fox PT, Miezin FM, Allman JM, Van Essen DC, Raichle ME. Retinotopic organization of human striate cortex mapped with positron emission tomography. *J Neurosci.* 1987;7:913-922.
8. Orr LS, Schatz NJ, Gonzalez CF, Savino PJ, Corbett JJ. Computerized axial tomography in evaluation of occipital lobe lesions. In: Smith JL, ed. *Neuro-ophthalmology Update.* New York, NY: Masson Publishing; 1977:351-367.
9. McCauley DL, Russell RWR. Correlation of CAT scan and visual field defects in vascular lesions of the posterior visual pathways. *J Neurol Neurosurg Psychiatry.* 1979;42:298-311.
10. Kattah JC, Dennis P, Kolsky MP, Schellinger D, Cohan SL. Computed tomography in patients with homonymous visual field defects: a clinico-radiologic correlation. *Comput Tomogr.* 1981;5:301-312.
11. Spector RH, Glaser JS, David NJ, Vining DQ. Occipital lobe infarctions: perimetry and computed tomography. *Neurology.* 1981;31:1098-1106.
12. Daniel PM, Whitteridge D. The representation of the visual field on the cerebral cortex in monkeys. *J Physiol (Lond).* 1961;159:203-221.
13. Van Essen DC, Newsome WT, Maunsell HR. The visual field representation in striate cortex of the macaque monkey: asymmetries, anisotropies, and individual variability. *Vision Res.* 1984;24:429-448.
14. Stensaas SS, Eddington DK, Dobelle WH. The topography and variability of the primary visual cortex in man. *J Neurosurg.* 1974;40:747-755.
15. Damasio H, Damasio AR. *Lesion Analysis in Neuropsychology.* New York, NY: Oxford University Press; 1989.
16. Hubel DH, Wiesel TN. Functional architecture of macaque monkey visual cortex. *Proc R Soc Lond B Biol Sci.* 1977;198:1-59.
17. Tamraz J. Neuroradiologic investigation of the visual system using magnetic resonance imaging. *J Clin Neurophysiol.* 1994;11:500-518.
18. McFadzean R, Brosnahan D, Hadley D, Mutlukan E. Representation of the visual field in the occipital striate cortex. *Br J Ophthalmol.* 1994;78:185-190.
19. Schneider W, Noll DC, Cohen JD. Functional topographic mapping of the cortical ribbon in human vision with conventional MRI scanners. *Nature.* 1993;365: 150-153.
20. Tootell RBH, Reppas JB, Kwong KK, et al. Functional analysis of human MT and related visual cortical areas using magnetic resonance imaging. *J Neurosci.* 1995; 15:3215-3230.
21. Sereno MI, Dale AM, Reppas JB, et al. Borders of multiple visual areas in humans revealed by functional magnetic resonance imaging. *Science.* 1995;268: 889-893.
22. Engel SA, Glover GH, Wandell BA. Retinotopic organization in human visual cortex and the spatial precision of functional MRI. *Cereb Cortex.* 1997;7:181-192.
23. Lai S, Hopkins AL, Haacke EM, et al. Identification of vascular structures as a major source of signal contrast in high resolution 2D and 3D functional activation imaging of the motor cortex at 1.5T: preliminary results. *Magn Reson Med.* 1993;30:387-392.
24. Polyak S. Modern investigation of the visual pathways and centers. In: Kluver H, ed. *The Vertebrate Visual System.* Chicago, Ill: University of Chicago Press; 1957: 163-203.
25. Polyak S. Clinical and pathoanatomical observations of cases with disturbances of the visual fields. In: Kluver H, ed. *The Vertebrate Visual System.* Chicago, Ill: University of Chicago Press; 1957:695-755.
26. Horton JC, Hocking DR. Relative magnification of the central visual field representation in striate cortex of macaques and humans. *Soc Neurosci Abstracts.* 1997;23:1945.

ARCHIVES Web Quiz

Be sure to visit the *Archives of Ophthalmology*'s World Wide Web site (http://www.ama-assn.org/ophth) and try your hand at our new Clinical Challenge interactive quiz. We invite visitors to make a diagnosis based on selected information from a case report or other feature scheduled to be published in the following month's print edition of the ARCHIVES. The first visitor to e-mail our Web editors with the first correct answer wins an *Archives of Ophthalmology* CD-ROM and will be recognized in the print journal and on our Web site. A full discussion of the case featured in the quiz can be found in the following month's print edition of the journal.

ARCHIVES Web Quiz Winner for December 1998:
Our congratulations to the winner of our Clinical Challenge, Iman Ezzat Ahmed Abu-elenein, MOphth, Alexandria, Egypt.